

# The phase transition and the Quasi-Normal Modes of black Holes

Jianyong Shen and Bin Wang\*

*Department of Physics, Fudan University, 200433 Shanghai*

Chi-Yong Lin†

*Department of Physics, National Dong Hwa University, Shoufeng, 974 Hualien*

Rong-Geng Cai‡

*Institute of Theoretical Physics, Chinese Academy of Sciences, P.O. Box 2735, 100080 Beijing*

Ru-Keng Su§

*China Center of Advanced Science and Technology (World Laboratory) P.O. Box 8730, 100080 Beijing and*

*Department of Physics, Fudan University, 200433 Shanghai*

We reexamined the argument that the quasinormal modes could be a probe of the phase transition of a topological black hole to a hairy configuration by investigating general scalar perturbations. We found further evidence in the quasinormal modes for this phase transition. For the general black hole configurations, we observed that although the quasinormal modes can present us different phases of different configurations, there is no dramatic change in the slope of quasinormal frequencies at the critical point of the phase transition. More detailed studies of quasinormal modes are needed to reveal the subtle behavior of the phase transition.

PACS numbers: 04.30.Nk, 04.70.Bw

## I. INTRODUCTION

Black holes' quasinormal modes (QNMs) have been an intriguing subject of discussions in the past decades [1, 2, 3]. The QNM is believed as characteristic sound of black holes, which describes the damped oscillations under perturbations in the surrounding geometry of a black hole with frequencies and damping times of the oscillations entirely fixed by the black hole parameters. The QNMs of black holes have potential astrophysical interest since it could lead to the direct identification of the black hole existence through gravitational wave observation to be realized in the near future[1, 2]. Despite the astrophysical interest, it has been argued that the black holes' QNM could be a testing ground for fundamental physics. Motivated by the discovery of the AdS/CFT correspondence, the investigation of QNM in anti-de Sitter(AdS) spacetimes became appealing in the past several years. It was argued that the QNMs of AdS black holes have direct interpretation in term of the dual conformal field theory(CFT)[3, 4, 5, 6, 7, 8, 9]. Attempts of using QNMs to investigate the dS/CFT correspondence have also been given[10]. Recently QNMs in asymptotically flat spaces have acquired further attention, since the possible connection between the classical vibrations of a black hole spacetime and various quantum aspects was proposed by relating the real part of the QNM frequencies to the Barbero-Immirzi(BI) parameter, a factor introduced by hand in order that loop quantum gravity reproduces correctly the black hole entropy [11]. The extension has been done in the dS background [12], however in the AdS black hole spacetime, the direct relation has not been found[13].

Recently further motivation of studying the QNMs has been pointed out in [14] by arguing that QNMs can reflect the black hole phase transition. By calculating the simplest possible QNMs of electromagnetic perturbations in the background of the MTZ black hole obtained in [15], it was claimed in [14] that they found the evidence of the phase transition in the QNMs behavior for small topological black holes with scalar hair. Further they claimed that at the critical temperature, the continuously matching of thermodynamical functions leads the phase transition to be of the second order and they gave the order parameter of the phase transition. Their result is interesting, since it might be the first phenomenon telling us the existence of the phase transition in black hole physics.

Is the obtained signature of phase transition in the QNMs of electromagnetic perturbation just an accident? Does

---

\*Electronic address: wangb@fudan.edu.cn

†Electronic address: lcyong@mail.ndhu.edu.tw

‡Electronic address: cairg@itp.ac.cn

§Electronic address: rksu@fudan.ac.cn

the connection between QNMs and phase transition hold for more general field perturbations such as the general scalar and gravitational perturbations? Can the QNMs be an effective probe of phase transitions in more general black hole configurations? In this paper we are trying to answer these questions. We will first extend the study in [14] by investigating the scalar perturbations around the MTZ black holes and computing its possible QNMs. MTZ black hole is an exact topological black hole solution wearing minimally coupled nontrivial scalar field. The study of the scalar perturbation in this black hole background is interesting. Numerically we will show that the change of slope of the QNMs again appears as we decrease the value of the horizon radius below the critical value as that in the electromagnetic perturbation [14] which shows the phase transition of a vacuum topological black hole to the MTZ black hole with scalar hair. To examine whether the QNM is an effective probe of the phase transition in general configurations, we will calculate the QNMs of scalar perturbation of the AdS black holes with Ricci flat horizons using AdS soliton as the background. It was found that there is a phase transition analogous to the Hawking-Page transition for AdS black holes [19, 20]. We are going to study whether the signature of this phase transition can be reflected in the QNMs behavior.

## II. THE TOPOLOGICAL BLACK HOLE WITH SCALAR HAIR

Considering the four-dimensional gravity with negative cosmological constant ( $\Lambda = -3/l^2$ ) and a scalar field described by the action

$$I = \int d^4x \sqrt{-g} \left[ \frac{R + 6l^{-2}}{16\pi G} - \frac{1}{2} \partial^\mu \phi \partial_\mu \phi - V(\phi) \right] \quad (1)$$

where the potential is given by  $V(\phi) = -\frac{3}{4\pi G l^2} \sinh^2 \sqrt{\frac{4\pi G}{3}} \phi$ , we have the equation of motion of gravitational field

$$G_{\mu\nu} + \Lambda g_{\mu\nu} = 8\pi G (\nabla_\mu \phi \nabla_\nu \phi - \frac{1}{2} g_{\mu\nu} (\nabla \phi)^2 - g_{\mu\nu} V(\phi)) \quad (2)$$

and the scalar field satisfying

$$\nabla^2 \phi - \frac{dV}{d\phi} = 0. \quad (3)$$

The exact solution of topological black hole with the scalar field can be found with the metric [15]

$$ds^2 = \frac{r(r + 2G\mu)}{(r + G\mu)^2} \left[ -\left(\frac{r^2}{l^2} - \left(1 + \frac{G\mu}{r}\right)^2\right) dt^2 + \left(\frac{r^2}{l^2} - \left(1 + \frac{G\mu}{r}\right)^2\right)^{-1} dr^2 + r^2 d\sigma^2 \right] \quad (4)$$

and the scalar field reads

$$\phi = \sqrt{\frac{3}{4\pi G}} \tanh^{-1} \frac{G\mu}{r + G\mu}. \quad (5)$$

Here  $d\sigma^2$  is the line element of the base manifold  $\Sigma$ , which has negative constant curvature [15]. The constant  $\mu$  stands for the mass of black hole. The range of  $r$  is taken as  $r > -2\mu$  for negative mass and  $r > 0$  otherwise to avoid the singularities of the curvature and the scalar field, where the conformal factor vanishes. The event horizon is given by

$$r_+ = \frac{l}{2} (1 + \sqrt{1 + 4G\mu/l}). \quad (6)$$

From Eq.(5), we can see that the black hole always wears a scalar field for fixed non-zero mass. When  $\mu = 0$ , the metric Eq.(4) stands for a locally AdS spacetime without the scalar field

$$ds^2 = -\left(\frac{r^2}{l^2} - 1\right) dt^2 + \left(\frac{r^2}{l^2} - 1\right)^{-1} dr^2 + r^2 d\sigma^2. \quad (7)$$

The interesting fact is that the above AdS spacetime can also be obtained from a topological black hole without scalar field

$$ds^2 = -\left(\frac{\rho^2}{l^2} - 1 - \frac{2G\mu}{\rho}\right) dt^2 + \left(\frac{\rho^2}{l^2} - 1 - \frac{2G\mu}{\rho}\right)^{-1} d\rho^2 + \rho^2 d\sigma^2, \quad (8)$$

when the mass  $\mu$  goes to zero. This means that for a given mass, there are two branches of different black hole solutions. By computing and comparing their free energies, Martinez *et al.* [15] suggested that a second order phase transition exists when the temperature (the even horizon) crosses a critical value  $T_c = \frac{1}{2\pi l}$  ( $r_c = l$ ). When  $T > T_c$  ( $r_+ > l$ ), both of black holes have positive mass. The black hole will absorb the scalar field dress and turn into the stabler bare one Eq.(8). When  $T < T_c$  ( $r_+ < l$ ), both of black holes have negative mass. A process of dressing up scalar field will happen for the bare black hole and the MTZ black hole has higher stability. Koutsoumbas *et al.* [14] further studied the behavior of the free energies of both black holes and related it to the order parameter defined by

$$\lambda = \begin{cases} \frac{T_0 - T}{T_0 + T}, & T < T_0 \\ 0, & T > T_0. \end{cases} \quad (9)$$

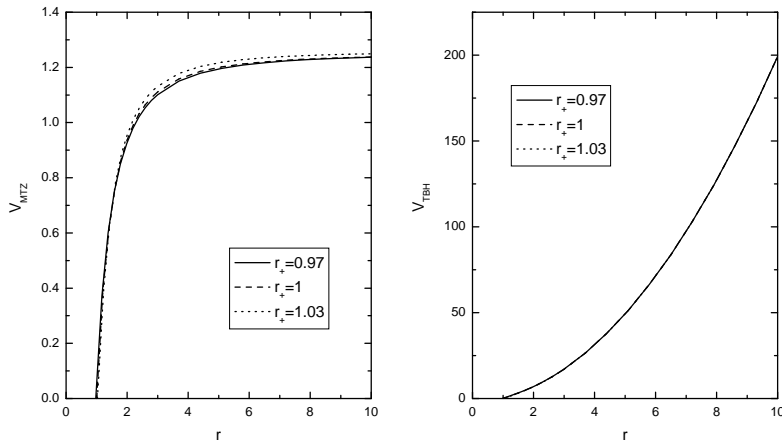


Figure 1: The effective potentials of the scalar perturbations. The left one stands for the MTZ black hole and the right for the topological back hole, when  $\xi = 1$  in the Eq.(17) and Eq.(20).

By computing the simplest possible QNMs of electromagnetic perturbation in the MTZ and TBH backgrounds, Koutsoumbas *et al.* [14] showed that near the critical temperature and for small black holes there is clear evidence in QNMs on the second order phase transition between the vacuum topological black hole and the MTZ black hole with scalar hair. It is of interest to generalize their study to QNMs of more general fields perturbations, such as the scalar field perturbation. In this subsection we calculate numerically the QNMs of scalar perturbation for both MTZ and topological black holes and examine the phase transition footprint.

Since the conformal factor in Eq.(4) does not play an important role, for the convenience of discussion and calculation, we make a conformal transformation to get rid of this factor and take  $8\pi G = 1$ ,  $l = 1$ . In this frame the field equations are [17]

$$(1 - \frac{1}{6}\phi^2)G_{\mu\nu} - 3g_{\mu\nu} = \frac{2}{3}\nabla_\mu\phi\nabla_\nu\phi - \frac{1}{6}g_{\mu\nu}(\nabla\phi)^2 + \frac{1}{3}g_{\mu\nu}\phi\nabla^2\phi - g_{\mu\nu}V(\phi) \quad (10)$$

and

$$\nabla^2\phi = \frac{2}{3}(-3 + V(\phi))\phi + (1 - \frac{1}{6}\phi^2)\frac{dV}{d\phi} \quad (11)$$

with

$$V(\phi) = \frac{1}{12}\phi^4. \quad (12)$$

Considering that all physical quantities are calculated in the new frame, the metric and the scalar field of MTZ black hole are now

$$ds^2 = -(r^2 - (1 + \frac{\mu}{r})^2)dt^2 + (r^2 - (1 + \frac{\mu}{r})^2)^{-1}dr^2 + r^2d\sigma^2 \quad (13)$$

and

$$\phi = \sqrt{6} \frac{\mu}{r + \mu}. \quad (14)$$

Expressing the perturbation of scalar field  $\tilde{\phi} = \phi + \delta\phi$ , we obtain the linear perturbation equation by varying  $\phi$  in Eq.(11)

$$\nabla^2 \delta\phi = \delta\phi \left[ \frac{1}{3} \phi \frac{dV}{d\phi} + \frac{2}{3} (V - 3) + \left(1 - \frac{1}{6} \phi^2\right) \frac{d^2 V}{d\phi^2} \right]. \quad (15)$$

When we consider the perturbation of the scalar field  $\tilde{\phi} = \phi + \delta\phi$ , in principle the back-reaction of the metric perturbation will affect the scalar field. However, the effect of the metric fluctuation on the perturbation of the scalar can be dropped near the critical point  $\mu = 0$ . To see this, let us consider a simple case where the perturbed metric is still of the form (13) and the metric function  $f = r^2 - (1 + \frac{\mu}{r})^2$  has a small fluctuation as  $\tilde{f} = f + \delta f(t, r)$ . Then linearizing the equation (11), we have

$$\nabla^2 \delta\phi + \left( \frac{2\phi'}{r} + \phi'' \right) \delta f + \phi' \delta f' = \delta\phi \left[ \frac{1}{3} \phi \frac{dV}{d\phi} + \frac{2}{3} (V - 3) + \left(1 - \frac{1}{6} \phi^2\right) \frac{d^2 V}{d\phi^2} \right]. \quad (16)$$

The last two terms in the left-hand-side of the above equation are contributions from the back-reaction of the metric perturbation. In our study, since our interest is focused on the QNMs near the critical point, it is easy to show that the factors of contributions from metric back-reaction tend to zero when  $\mu \rightarrow 0$  at the critical point by using (14). Thus the back-reaction due to the metric perturbation can be neglected when we focus on the behavior of the scalar perturbations around the critical point  $\mu = 0$ . Also near this point, the first and third terms in the right hand side of the equation can be neglected. As a result, near the critical point, the expression in the square brackets in the right hand side of (15) turns to be  $-2$ . Further, let us notice that the scalar field in the frame (13) is a conformal scalar. This might explain that although the two potentials shown in Fig. 1 look different, the numerical results of the QNMs for two black holes are quite similar (see Fig. 2 and 3). Of course, we may consider a scalar perturbation, which is not related to the scalar field  $\phi$  in the black hole solution. In that case, we can obtain similar results for both black holes.

By the variable separation  $\delta\phi = \frac{1}{r} R(r) Y(\Sigma) e^{-i\omega t}$ , Eq.(15) is written as

$$\begin{aligned} R \{ \omega^2 - V_{MTZ} \} + R' f f' + R'' f^2 &= 0, \\ V_{MTZ} &= \left( \xi^2 + \frac{1}{4} \right) \frac{f}{r^2} - f(2 - \phi^2) + \frac{f f'}{r}. \end{aligned} \quad (17)$$

where  $f = r^2 - (1 + \frac{\mu}{r})^2$  and  $\xi^2 + 1/4$  is the eigenvalue of the harmonic function  $Y(\Sigma)$  on the hyperbolic space [16]. Taking  $R(r) = \tilde{R}(r) e^{-i\omega r_*}$  with  $dr_* = dr/f$ , we can rewrite Eq.(17) into

$$\tilde{R} \left\{ -\left( \xi^2 + \frac{1}{4} \right) \frac{1}{r^2} + (2 - \phi^2) - \frac{f'}{r} \right\} + \tilde{R}' (f' - 2i\omega) + \tilde{R}'' f = 0. \quad (18)$$

For the topological black hole Eq.(8), the scalar perturbation is just described by the Klein-Gorden equation

$$\nabla^2 \delta\phi = 0 \quad (19)$$

which, under the variable separation  $\delta\phi = \frac{1}{r} R(r) Y(\Sigma) e^{-i\omega t}$  and the transformation  $R(r) = \tilde{R}(r) e^{-i\omega r_*}$  with  $dr_* = dr/g$ , it can be expressed as

$$\begin{aligned} -\frac{V_{TBH}}{f_1} \tilde{R} + \tilde{R}' (f'_1 - 2i\omega) + \tilde{R}'' f_1 &= 0, \\ V_{TBH} &= f_1 \left[ \left( \xi^2 + \frac{1}{4} \right) \frac{1}{r^2} + \frac{f'_1}{r} \right]. \end{aligned} \quad (20)$$

Here the metric coefficient  $f_1 = r^2 - 1 - \frac{2\mu}{r}$ .

The behaviors of effective potentials of scalar perturbations in the MTZ and topological black holes' backgrounds are shown in Fig.1. Compared with the situation in the topological black hole, the effective potential in the MTZ background does not diverge, but converges to a nonzero constant at spatial infinity, due to the compensation of the divergence of the non-zero scalar field in Eq.(17). For the convergent potential at spatial infinity, Koutsoumbas *et al.*

[14] imposed the boundary condition that the wave function of the electromagnetic perturbation vanishes at spatial infinity and employed the numerical method devised by Horowitz and Hubeny [4] in the MTZ background. In our case, we can see that the tortoise coordinate  $r_*$  tends to a constant for big  $r$  in the MTZ background, which is similar to that of the Schwarzschild-AdS observed in [18]. This leads  $e^{-i\omega r_*}$  to be a constant for big  $r$ , which indicates that there is no flux at spacial infinity. As for  $\tilde{R}(r)$ , we can obtain the approximate solution  $\tilde{R} \sim e^{x \cdot Const.}$  after substituting  $r$  with  $1/x$  in Eq.(18) and taking the leading terms near  $x = 0$ . Therefore  $\tilde{R}$  is also a constant at the spacial infinity  $x = 0$ . In other words, the oscillation of the QNMs is frozen, hence the wave vanishes at the infinity and this constant can be set zero by the definition of QNM. This makes us confident to employ the method of Horowitz and Hubeny to calculate the QNMs of the MTZ black hole. For the topological black hole case, Horowitz and Hubeny method applies naturally.

In the following we present our numerical results of QNMs for the MTZ and topological black holes when their event horizons cross the critical point  $r_c = 1$ , e.g.  $r_+ = 0.97, 1, 1.03$ . Our results of are shown in Fig.2 and Fig.3 respectively.

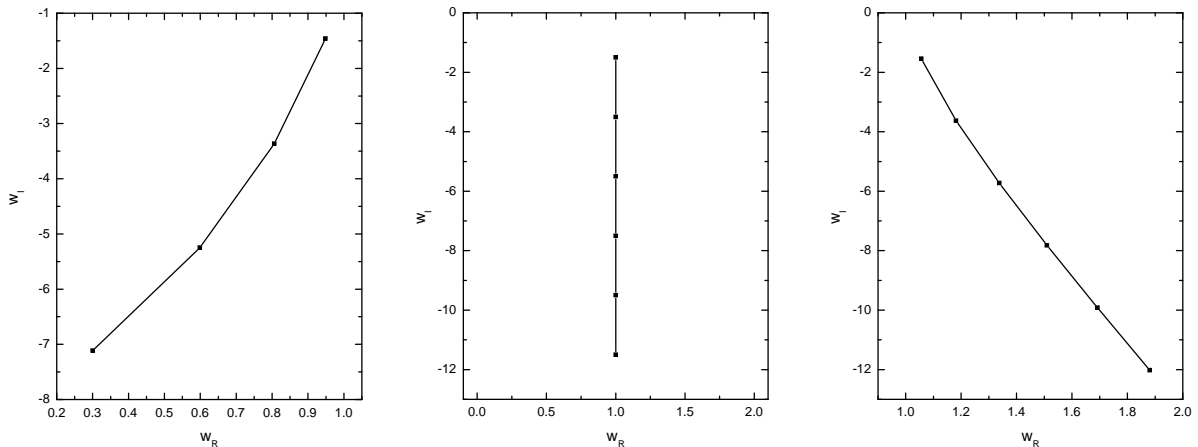


Figure 2: The QNMs of scalar perturbations in the MTZ black hole. The results are calculated with  $\xi = 1$  in the Eq.(18). The right, middle and left figures stand for the cases of  $r_+ = 0.97, 1.00$  and  $1.03$ , respectively.

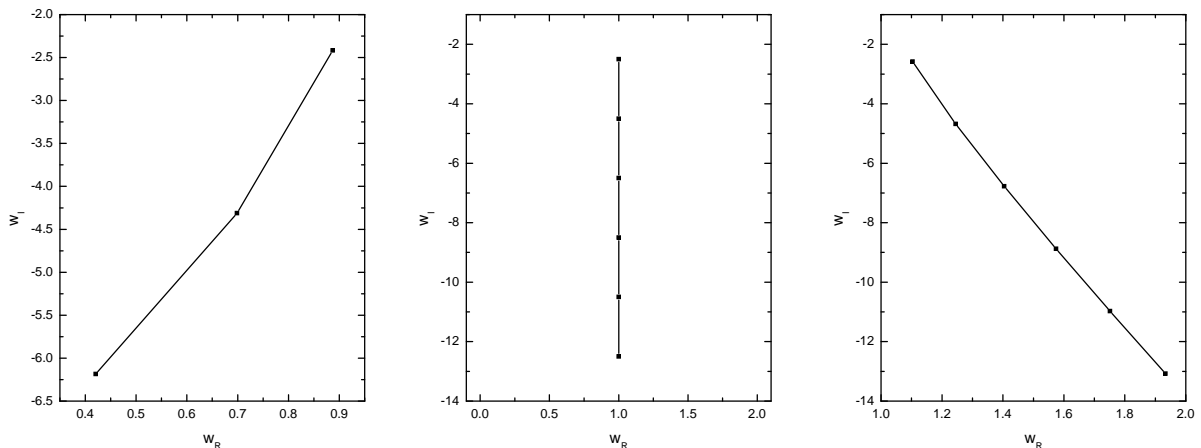


Figure 3: The QNMs of scalar perturbation in the topological black hole. The results are calculated with  $\xi = 1$  in the Eq.(20). The right, middle and left figures stand for the cases of  $r_+ = 0.97, 1.00$  and  $1.03$ , respectively.

We can see that when  $r_+ < 1$ , the slope of QNMs is positive and the slope tends to minus infinity as we approach

$r_+ = 1$ . When  $r_+ > 1$ , the QNMs lie on a straight line with negative slope. The results of the QNMs of scalar perturbation present us very similar properties to those in the electromagnetic perturbations [14]. As argued in the study of the electromagnetic perturbation, the change of slope of the QNMs in the scalar perturbations as we decrease the value of the horizon radius below a critical value reveals the phase transition of a vacuum topological black hole to the MTZ hole with scalar hair. Our result presents a support to [14] in the study of the phase transition for the four-dimensional topological black holes with scalar hair.

### III. ADS BLACK HOLES WITH RICCI FLAT HORIZONS ON THE ADS SOLITON BACKGROUND

To investigate whether the QNMs is an effective tool to disclose phase transition in general black hole configurations, we are going to extend the discussion to phase transitions for flat AdS black holes in this section. Thermodynamics of AdS black holes with Ricci flat horizons using the AdS soliton as the thermal background has been investigated in [19, 20]. It was found that there is a phase transition analogous to the Hawking-Page transition. We will compute the QNMs of the scalar perturbation in the flat AdS black hole and AdS soliton backgrounds and examine whether the phase transition imprints in the QNMs.

The metric of the AdS black hole with Ricci flat horizon (flat AdS black hole) is [20]

$$ds_{bh}^2 = -V_b dt_b^2 + V_b^{-1} dr^2 + r^2 d\phi_b^2 + r^2 h_{ij} d\theta_i d\theta_j, \quad (21)$$

where

$$V_b = r^2 - \frac{k_b^{n-1}}{r^{n-3}} \quad (22)$$

with  $l = 1$  for simplicity.  $h_{ij}$  is a Ricci flat metric and  $\phi_b$  is identified with period  $\eta_b$ .  $k_b$  is the black hole mass parameter. The horizon is at  $V_b(r_{b+}) = 0$  and the zeros of  $V_b(r)$  are given by  $r_{b+}^{n-1} = k_b^{n-1}$ . By the analytical continuation  $t_b \rightarrow i\phi_s$  and  $\phi_b \rightarrow t_s$ , the AdS soliton is got

$$ds_s^2 = -r^2 dt_s^2 + V_s^{-1} dr^2 + V_s d\phi_s^2 + r^2 h_{ij} d\theta_i d\theta_j, \quad (23)$$

where  $V_s$  is the function Eq.(22) with  $k_s$  replacing  $k_b$ . To meet the requirement of regularity,  $r \geq r_{s+} k_s$ , where  $V_s(r_{s+})$  vanishes and  $\phi_s$  is identified with the period  $\beta_s = \frac{4\pi}{3r_{s+}}$ .

To calculate the energy and to study their thermodynamics, the standard regularization scheme is used[20], in which these two solutions are matched at a finite cutoff radius  $R$

$$\beta_b \sqrt{V_b} = R\eta_s, \quad \beta_s \sqrt{V_s} R\eta_b \quad (24)$$

and then the limit  $R \rightarrow \infty$  is taken after all quantities are calculated. By comparing the energies and the Euclidean actions of the two solutions, Surya et.al. [20] suggested a phase transition for  $n > 3$  analogous to the Hawking-Page transition. If  $k_b \ll k_s$ , small hot black hole is unstable and decays to small hot soliton, while large cold black hole is stable with  $k_b \gg k_s$ . In case of  $k_b \sim k_s$ , black hole is in equilibrium with the soliton including cases when they are large and hot, or cold and small.

In order to see the signature of this phase transition in QNMs, we study the scalar perturbations in these two solutions with the dimension  $n = 4$ . By separating variables  $\psi_b R_b(r, t) \Phi_b(\phi_b) Y(\theta)$  in the KG equation  $\nabla^2 \psi_b = 0$  of the flat AdS black hole Eq.(21), we have

$$\frac{R_b}{r^2} \left\{ \frac{1}{\Phi_b} \frac{d^2 \Phi_b}{d\phi_b^2} + \frac{1}{Y} \frac{d^2 Y}{d\theta^2} \right\} + \left( \frac{2V_b}{r} + V_b' \right) \frac{\partial R_b}{\partial r} + V_b \frac{\partial^2 R_b}{\partial r^2} - \frac{1}{V_b} \frac{\partial^2 R_b}{\partial t^2} = 0. \quad (25)$$

The second term of the square bracket just stands for the free motion in the  $\theta$  direction and then its eigenvalue is the kinetic energy  $-k^2$  with any real number  $k$ . The first term also can be considered as the free motion in the periodic coordinate  $\phi_b$ , therefore the eigenvalue is not a real number but discrete  $-\sigma_b^2 = -\left(\frac{2\pi n}{\eta_b}\right)^2$  ( $n = 0, 1, 2, \dots$ ). Taking Eq.(24) at the infinity  $R \rightarrow \infty$

$$\sigma_b^2 = \left( \frac{2\pi n}{\eta_b} \right)^2 \left( \frac{2\pi n}{\beta_s} \right)^2, \quad (26)$$

Eq.(25) can be written as

$$-\frac{R_b}{r^2} (\sigma_b^2 + k^2) + \left( \frac{2V_b}{r} + V_b' \right) \frac{\partial R_b}{\partial r} + V_b \frac{\partial^2 R_b}{\partial r^2} - \frac{1}{V_b} \frac{\partial^2 R_b}{\partial t^2} = 0. \quad (27)$$

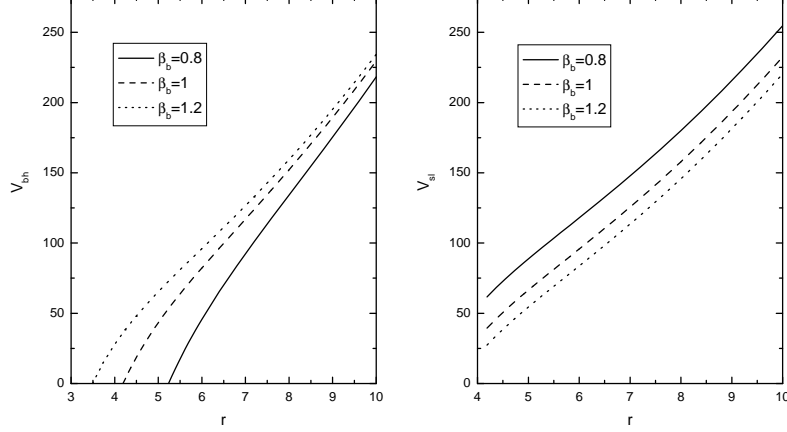


Figure 4: The effective potentials of the scalar perturbations. The left one stands for the flat AdS black hole and the right for the AdS soliton, when  $k = 1$ ,  $n = 1$  and  $\beta_s = 1$  fixed in the Eq.(28) and Eq.(30).

Setting  $R_b(t, r) = \frac{1}{r} \tilde{R}_b(r) e^{-i\omega t}$ , the above equation changes into

$$\begin{aligned}
 -\tilde{R}_b \{-\omega^2 + V_{bh}\} + V_b' V_b \tilde{R}_b' + V_b^2 \tilde{R}_b'' &= 0, \\
 V_{bh} &= \frac{2V_b V_b'}{r} + \frac{V_b}{r^2} (\sigma_b^2 + k^2).
 \end{aligned} \tag{28}$$

Near the horizon  $r_{b+} = kb$ , the wave can be expanded as  $\tilde{R}_b(r) = \sum a_i^{(b)} (r - r_{b+})^{\rho+i}$  and the index  $\rho = \pm \frac{i\omega}{3r_{b+}}$  through the index equation. The effective potential  $V_{bh}$  is shown in Fig.4 which diverges at the spacial infinity. Because there only exists the ingoing wave near the horizon, the positive sign in  $\rho$  is discarded.

In the case of the AdS soliton Eq.(23), we follow the similar steps to that of the flat AdS black hole with the variable separation  $\psi_s = R_s(r, t) \Phi_s(\phi_s) Y(\theta)$  in KG equation and obtain

$$R_s \left\{ \frac{1}{V_s} \frac{1}{\Phi_s} \frac{d^2 \Phi_s}{d\phi_s^2} + \frac{1}{r^2} \frac{1}{Y} \frac{d^2 Y}{d\theta^2} \right\} + \left( \frac{2V_s}{r} + V_s' \right) \frac{\partial R_s}{\partial r} + V_s \frac{\partial^2 R_s}{\partial r^2} - \frac{1}{r^2} \frac{\partial^2 R_s}{\partial t^2} = 0. \tag{29}$$

As above, the eigenvalues of the second and first terms are  $-k^2$  and  $-\sigma_s^2 = -\left(\frac{2\pi n}{\eta_s}\right)^2$  ( $n = 0, 1, 2, \dots$ ) respectively. Hence the radial part of KG equation in the AdS soliton background is

$$\begin{aligned}
 -\tilde{R}_s \left\{ -\frac{\omega^2 V_s}{r^2} + V_{sl} \right\} + V_s' V_s \tilde{R}_s' + V_s^2 \tilde{R}_s'' &= 0, \\
 V_{sl} &= \frac{2V_s' V_s}{r} + \sigma_s^2 + \frac{k^2 V_s}{r^2}
 \end{aligned} \tag{30}$$

with  $R_s(t, r) = \frac{1}{r} \tilde{R}_s(r) e^{-i\omega t}$  and

$$\sigma_s^2 = \left( \frac{2\pi n}{\eta_s} \right)^2 \left( \frac{2\pi n}{\beta_b} \right)^2. \tag{31}$$

Again, the index  $\rho$  in the expansion  $\tilde{R}_s(r) = \sum a_i^{(s)} (r - r_{s+})^{\rho+i}$  is given by  $\rho = \pm \frac{\sigma_s}{3r_{s+}}$ . The negative sign is discarded to keep the convergence of the wave near the horizon  $r_{s+}$ . We plot  $V_{sl}$  in Fig.4 as the comparison to  $V_{bh}$ . Notice that the real index  $\rho$  is the main difference from that of the flat AdS black hole which indicates there is no wave flux near the boundary  $r_{s+}$ . In the far region, the AdS soliton approaches the AdS spacetime and hence no wave can flow to the infinity. Therefore, only normal modes exist similar to the form of stationary waves in the AdS soliton background, once some perturbations are excited. Our following numerical calculation proves this effect.

We still employ the method of Horowitz and Hubney to calculate the numerical QNMs of the flat AdS black hole and AdS soliton. We do the computation with  $k = 1$  and  $n = 1$  in Eq.(28) and Eq.(30), because the free motion in the

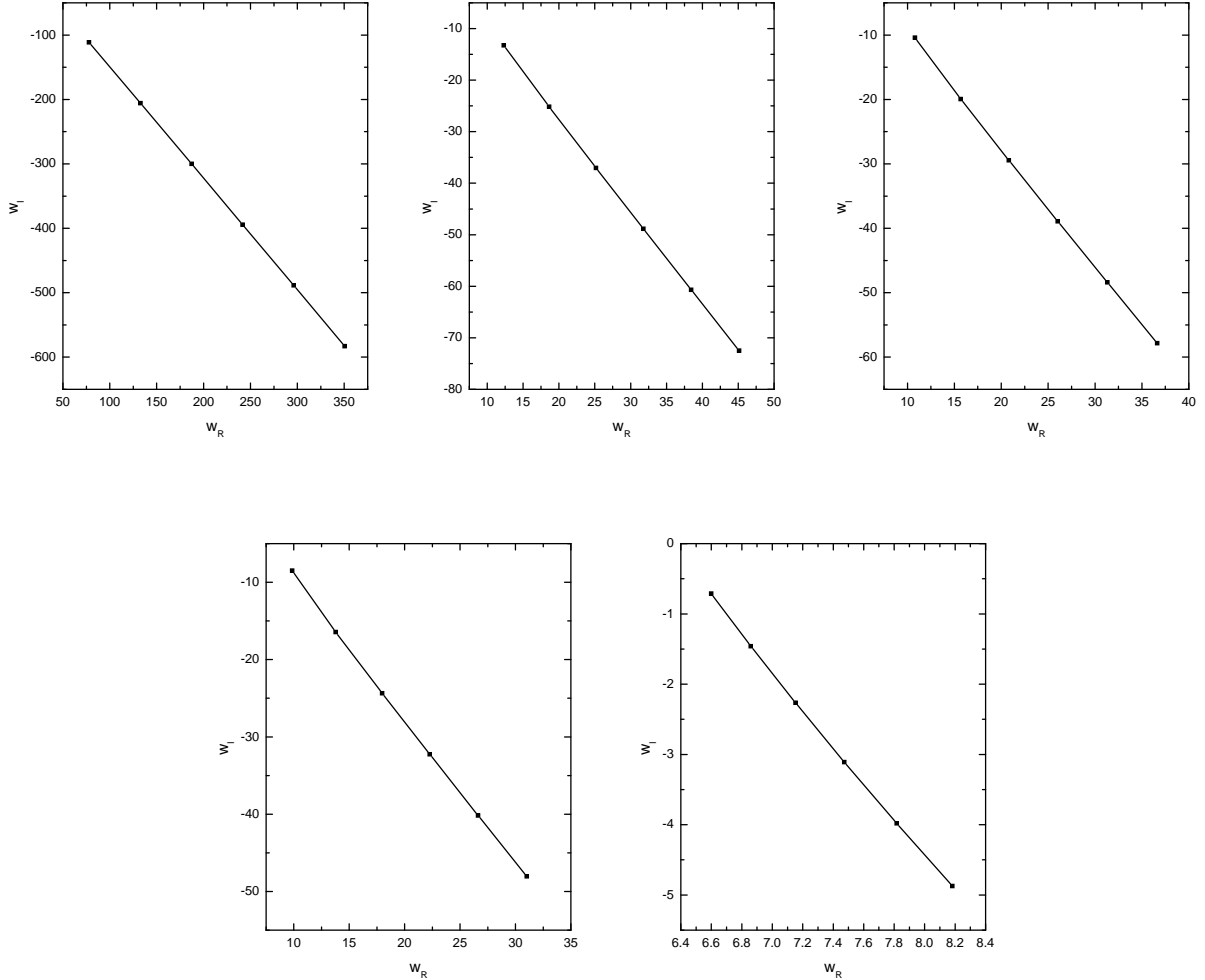


Figure 5: The QNMs of scalar perturbation in the flat AdS black hole. The results are calculated with  $k = 1$  and  $n = 1$  in Eq.(28). The right, middle and left figures in the first row stand for the cases of  $\beta_b = 0.1, 0.8$  and  $1.0$  respectively and the right and left ones in the second row for  $\beta_b = 1.2$  and  $10$

$\theta$  direction is not of importance and it is better that the wave number  $n$  of the motion in the  $\phi_\alpha$  ( $\alpha = b, s$ ) direction does not vanish if we consider the more differences between the flat AdS black hole and AdS soliton in the QNMs. During the computation, we fix the period  $\beta_s = 1.0$  and vary  $\beta_b$  from  $0.1$  to  $10$  representing the cases where  $\beta_b$  is much smaller to much bigger than  $\beta_s$  in order to satisfy the condition of the phase transition. Fig.5 and Table.I show the QNMs of the scalar perturbation in the two spacetimes. The QNMs in the flat AdS black hole always have negative slope in the  $w_R - w_I$  diagrams, distinguished from the situation of the MTZ-TBH phase transition. As for the AdS soliton background, there only exist the normal modes as we expected and no special events happen here. We can see that flat AdS black hole and AdS soliton are staying in different phases as disclosed by the QNMs behavior, however the phase transition as revealed in [20] occurring around the critical point  $\beta_b \sim \beta_s = 1$  does not imprint explicitly in the present QNMs study. More detailed analysis is called for to reveal more subtle changes in the QNMs due to this phase transition.

#### The Normal Modes $\omega$



$\beta_b = 0.1$	118.869	214.033	308.428	402.572	496.607	590.583
$\beta_b = 0.8$	19.381	31.108	42.835	54.563	66.293	78.022
$\beta_b = 1$	16.590	25.921	35.278	44.646	54.019	63.396
$\beta_b = 1.2$	14.743	22.475	30.250	38.042	45.844	53.652
$\beta_b = 10$	7.097	7.855	8.662	9.498	10.356	11.228

Table I

*The normal modes of the scalar field in the AdS soliton background with fixed  $\beta_s = 1$ .*

#### IV. CONCLUSIONS AND DISCUSSIONS

Because of its astrophysical and theoretical interests, the QNMs of black holes has been an intriguing subject of discussions. Calculating the QNMs of electromagnetic perturbations of the MTZ and topological black holes, Koutsoumbas et al[14] argued that the QNMs imprints the phase transition of a vacuum topological black hole to the MTZ black hole with scalar hair. To examine whether this interesting result is just an accident, we have studied the QNMs for the general scalar perturbations. We observed in the numerical investigation that the slope of the QNMs changes as we decrease the value of the horizon radius below a critical value, which is in agreement with the behavior observed for the electromagnetic perturbations[14]. Thus for the four-dimensional topological black holes with scalar hair, the QNMs really presents the signature of the phase transition.

It would be fair to say that we just have the thermodynamical descriptions of the black holes' phase transitions, the physical phenomenons of the phase transitions are not clear. If the QNMs can probe the phase transition as disclosed in topological black holes with scalar hair, it would be interesting to ask whether this tool is effective for general black hole configurations. We have investigated the QNMs of the scalar perturbations in the backgrounds of flat AdS black holes and AdS solitons. Although it is clear from the QNMs that flat AdS black holes and AdS solitons are in different phases, it is not clear as observed in MTZ and topological black holes that near the critical point there is a sudden change in the QNMs behavior. More detailed careful study of QNMs is called for to disclose more subtle changes in the QNMs caused by the phase transition.

#### Acknowledgments

This work was partially supported by NNSF of China, Ministry of Education of China and Shanghai Education Commission. JY Shen was supported by the Fudan Creative Fund for Graduate Student.

- 
- [1] H. P. Nollert, *Class. Quant. Grav.* 16, R159 (1999).  
[2] K. D. Kokkotas and B. G. Schmidt, *Living Rev. Rel.* 2, 2 (1999).  
[3] B. Wang, *Braz. J. Phys.* 35, 1029 (2005).  
[4] G. T. Horowitz and V. E. Hubeny, *Phys. Rev. D* 62, 024027 (2000).  
[5] B. Wang, C.Y. Lin, and E. Abdalla, *Phys. Lett. B* 481, 79 (2000); B. Wang, C. Molina, and E. Abdalla, *Phys. Rev. D* 63, 084001 (2001); J.M. Zhu, B. Wang, and E. Abdalla, *Phys. Rev. D* 63, 124004 (2001).  
[6] V. Cardoso and J.P.S. Lemos, *Phys. Rev. D* 63, 124015 (2001); V. Cardoso and J.P.S. Lemos, *Phys. Rev. D* 64, 084017(2001); E. Berti and K.D. Kokkotas, *Phys. Rev. D* 67, 064020 (2003); V. Cardoso and J.P.S. Lemos, *Class. Quantum Grav.* 18, 5257 (2001); E. Winstanley, *Phys. Rev. D* 64, 104010 (2001); J. Crisostomo, S. Lepe and J. Saavedra, *Class.Quant.Grav.* 21 (2004) 2801-2810; S. Lepe, F. Mendez, J. Saavedra, L. Vergara, *Class.Quant.Grav.* 20 (2003) 2417-2428.  
[7] D. Birmingham, I. Sachs, S. N. Solodukhin, *Phys.Rev.Lett.* 88 (2002) 151301; D. Birmingham, *Phys.Rev. D* 64 (2001) 064024.  
[8] B. Wang, E. Abdalla and R. B. Mann, *Phys. Rev. D* 65, 084006 (2002); J.S.F. Chan and R.B. Mann, *Phys. Rev. D* 59, 064025 (1999).  
[9] S. Musiri, G. Siopsis, *Phys.Lett. B* 576 (2003) 309-313; R. Aros, C. Martinez, R. Troncoso, J. Zanelli, *Phys.Rev. D* 67 (2003) 044014; A. Nunez, A. O. Starinets, *Phys.Rev. D* 67 (2003) 124013.  
[10] E. Abdalla, B. Wang, A. Lima-Santos and W. G. Qiu, *Phys. Lett. B* 538, 435 (2002); E. Abdalla, K. H. Castello-Branco and A. Lima-Santos, *Phys. Rev. D* 66, 104018 (2002).  
[11] S. Hod, *Phys. Rev. Lett.* 81, 4293 (1998); A. Corichi, *Phys. Rev. D* 67, 087502 (2003); L. Motl, gr-qc/ 0212096; L. Motl and A. Neitzke, hep-th/0301173; A. Maassen van den Brink, gr-qc/0303095; J. Baez, gr-qc/0303027; O. Dreyer, *Phys. Rev.*

- Lett. 90, 08130 (2003); G. Kunstatter, Phys. Rev. Lett. 90, 161301 (2003); N. Andersson and C. J. Howls, gr-qc/0307020; V. Cardoso, J. Natario and R. Schiappa, hep-th/0403132.
- [12] V. Cardoso and J. P. S. Lemos, Phys. Rev. D 67, 084020 (2003); K. H. C. Castello-Branco and E. Abdalla, gr-qc/0309090.
  - [13] B. Wang, C.Y. Lin and C. Molina, Phys.Rev. D70 (2004) 064025
  - [14] G. Koutsoumbas, S. Musiri, E. Papantonopoulos, G. Siopsis, JHEP 0610 (2006) 006
  - [15] C. Martinez, R. Troncoso and G. Zanelli, Phys. Rev. D70 (2004) 084035.
  - [16] A. Terras, *Harmonic Analysis on Symmetric spaces and Applications I* (Springer-Verlag, New York, 1985)
  - [17] E. Winstanley, *Found.Phys.* **33**, (2003) 111
  - [18] J. Natario, R. Schiappa, Adv.Theor.Math.Phys. 8 (2004) 1001.
  - [19] G. T. Horowitz and R. C. Myers, *Phys.Rev.* **D59**, (1999) 026005
  - [20] S. Surya, K. Schleich and D. M. Witt, *Phys.Rev.Lett.* **86**, (2001) 5231